

A Hinge-Free, Non-Restrictive, Lightweight Tethered Exosuit for Knee Extension Assistance During Walking

Evelyn J. Park, Tunc Akbas, Asa Eckert-Erdheim, Lizeth H. Sloot, Richard W. Nuckols¹, Dorothy Orzel¹, Lexine Schumm, Terry D. Ellis, Louis N. Awad², and Conor J. Walsh¹, *Member, IEEE*

Abstract—In individuals with motor impairments such as those post-stroke or with cerebral palsy, the function of the knee extensors may be affected during walking, resulting in decreased mobility. We have designed a lightweight, hinge-free wearable robot combining soft textile exosuit components with integrated rigid components, which assists knee extension when needed but is otherwise highly transparent to the wearer. The exosuit can apply a wide range of assistance profiles using a flexible multi-point reference trajectory generator. Additionally, we implemented a controller safety limit to address the risk of hyperextension stemming from the hinge-free design. The exosuit was evaluated on six healthy participants walking uphill and downhill on a treadmill at a 10° slope with a set of joint power-inspired assistance profiles. A comparison of sagittal plane joint angles between no exosuit and exosuit unpowered conditions validated the device transparency. With positive power assistance, we observed reduction in average positive knee biological power during uphill walking (left: $17.5 \pm 3.21\%$, $p = 0.005$; right: $23.2 \pm 3.54\%$, $p = 0.008$). These initial findings show promise for the assistive capability of the device and its potential to improve the quality of gait and increase mobility in clinical populations.

Index Terms—Wearable robotics, exoskeletons, exosuit, knee, gait biomechanics.

Manuscript received October 31, 2019; revised February 19, 2020; accepted April 15, 2020. Date of publication April 21, 2020; date of current version May 20, 2020. This article was recommended for publication by Associate Editor C. Riviere and Editor P. Dario upon evaluation of the reviewers' comments. This work was supported in part by the National Institutes of Health Bioengineering Research Grants under Grant R01HD088619, in part by the Wyss Institute for Biologically Inspired Engineering, and in part by the Harvard School of Engineering and Applied Sciences. (*Corresponding author: Evelyn J. Park.*)

Evelyn J. Park, Tunc Akbas, Asa Eckert-Erdheim, Richard W. Nuckols, Dorothy Orzel, Lexine Schumm, and Conor J. Walsh are with the School of Engineering and Applied Sciences, Harvard University, Cambridge, MA 02138 USA, and also with the Wyss Institute for Biologically Inspired Engineering, Harvard University, Cambridge, MA 02138 USA (e-mail: ejpark@g.harvard.edu; tuncakbas@g.harvard.edu; asa.eckert-erdheim@wyss.harvard.edu; rnuckols@g.harvard.edu; dorothy.orzel@wyss.harvard.edu; lschumm@g.harvard.edu; walsh@seas.harvard.edu).

Lizeth H. Sloot is with the Institute for Computer Engineering (ZITI), Heidelberg University, 69117 Heidelberg, Germany (e-mail: lizeth.sloot@ziti.uni-heidelberg.de).

Terry D. Ellis and Louis N. Awad are with the Department of Physical Therapy and Athletic Training, Sargent College, Boston University, Boston, MA 02215 USA (e-mail: tellis@bu.edu; louawad@bu.edu).

Digital Object Identifier 10.1109/TMRB.2020.2989321

I. INTRODUCTION

KNEE extensors contribute to both support and forward propulsion during gait [1]. In healthy locomotion, knee extension assistance could help off-load the knee extensor muscles, reducing fatigue and therefore the risk of fatigue-related knee injuries, and reduce loading on the knee joint. Individuals with neuromuscular disorders such as stroke or cerebral palsy (CP) exhibit altered dynamics at the knee during locomotion which affect performing activities of daily living. For instance, compensatory knee hyperextension following stroke results in reduced gait speed [2], increased energy expenditure [3], and long term joint pain [4]. On the other hand, excessive knee flexion such as in CP crouch gait leads to a decline in functional capability and loss of mobility [5]. Providing knee extension assistance could improve the ability of patients with knee deficits to load their affected limb(s), maintain stability during the stance phase of gait, and improve overall mobility. Knee extension support could also reduce energy expenditure during tasks requiring high loading of supporting limb(s), such as sit-to-stand transfers [6] and stairs [7], [8]. Furthermore, if the assistance is provided early in the rehabilitation process, it may help prevent the development of spasticity [9] and abnormal inter-joint couplings [10], [11] during gait.

Passive orthotics of the kind typically used in the clinic are limited in how they can benefit the knee. Knee-ankle-foot orthoses (KAFOs) rigidly lock the knee joint to prevent limb collapse, but this locking also causes users to resort to abnormal and energetically expensive gait compensations for the foot to clear the ground in swing [12], [13]. Stance control KAFOs do exist which can temporarily unlock and allow flexion during swing, but this binary locking/unlocking still falls short of the dynamic behavior of the knee in healthy locomotion.

Active robotic assistive devices can potentially address this gap, but despite the rapid advancement of the field in recent years, there are still many open questions surrounding knee assistance. Perhaps due to the knee joint's relatively low contribution to the overall limb power production during level ground walking [14], in-depth, systematic studies of robotic assistance in healthy locomotion have mostly focused instead on the ankle or the hip joint. For example, at the ankle alone, exoskeleton studies have examined everything from varying magnitude and/or timing of assistance [15],

to negative vs. positive power assistance [16], to net work rate vs. torque-based assistance [17], to automatic real-time tuning of assistance using optimization algorithms [18]. Of existing knee devices, many are designed not necessarily to assist, but to serve as experimental platforms for basic science studies, e.g., linking ankle plantarflexion with knee flexion to emulate the biarticular gastrocnemius muscle [19], or estimating knee impedance by applying controlled perturbations [20].

However, some recent studies appear to indicate that knee assistance may be beneficial for tasks where the joint experiences higher loads. For example, a combination knee and hip exoskeleton [21] tested in incline walking went from incurring a metabolic penalty with only the hip assistance activated, to achieving 8.8% metabolic reduction after knee assistance was added ($n = 2$). Another knee exoskeleton [22] achieved a 4.2% metabolic reduction in incline walking while carrying loads ($n = 4$). While these preliminary results are promising, they are limited in how much they reveal about the impact of knee assistance on user biomechanics: the former study examined multi-joint assistance but not knee-only assistance, while the latter did not report assistance profiles as this data was not available from the commercial exoskeleton that was used.

Similarly, few research studies have examined the biomechanical effects of knee exoskeleton assistance in clinical populations. While many commercial robotic knee devices exist for gait rehabilitation and assistance for individuals with neuromuscular injuries, such as the WelWalk (Toyota Motor Corporation, Japan), Tibion Bionic Leg (AlterG Inc., USA), Keeogo DermoSkeletoN (B-Temia Inc., Canada), and the C-brace (Ottobock, Germany), commercial devices such as these rarely publish details of their assistance method and generally focus device evaluation on high-level clinical metrics. While research devices typically place more emphasis on biomechanics, few knee devices have completed multi-subject evaluations. In one recent study, an exoskeleton providing knee extension assistance to children with CP demonstrated benefits such as reduced excessive knee flexion (crouch gait) during stance [23]. Another robotic knee orthosis applied knee flexion torque in post-stroke users with stiff knee gait, aiming to increase swing knee flexion in order to reduce ground clearance compensations such as circumduction. While the assistance did increase peak knee flexion, hip abduction increased as well, suggesting an abnormal coupling between the two [11]. This counter-intuitive result highlights how even seemingly straightforward hypotheses on a knee exoskeleton's impact may not hold true, and how there are still many unknowns affecting the impact of assistance. The lack of in-depth understanding in both clinical and healthy populations of the neuromuscular and biomechanical effects of different knee assistance profiles motivates further investigation.

With this work, our goal was to develop a flexible experimental platform for lab-based exploration of the effect of varying knee extension assistance on user biomechanics. To ensure that biomechanical responses due to changes in active assistance are not confounded by passive effects of the hardware, it was important for the device to be comfortable and natural to walk in, with minimal impact on walking

kinematics when unpowered. This meant that the device needed to be lightweight overall, to minimize added inertia on the legs, but also to be well-aligned with the user's knee joint. Misalignment can create high interaction forces [24], which could alter the wearer's natural gait and/or create discomfort at the interfaces. However, achieving good alignment is challenging: while the knee joint is often treated as a hinge joint with only 1 degree of freedom, it is actually more complex, sliding and rolling such that the joint center shifts over the range of motion (ROM) [25].

There are various ways in which exoskeletons address this issue. One is custom fabrication of the interface components, as in the case of KAFO-based devices [26], [27]. However, this increases cost and requires re-fabrication if the wearer undergoes physical changes, such as growth or changes in weight. Alternatively, mechanical design approaches may be used, such as complex linkages that better replicate the motion of the knee joint center [28], [29], or flexible structures that allow compliance in selected directions to take up misalignment [30]. However, few exoskeletons have actually evaluated whether they truly avoid unnaturally constraining or otherwise impacting the wearer's gait. To the best of our knowledge, the only previous devices that have done such validation for healthy walking are a quasi-passive knee exoskeleton [31] which compared the group-level mean angle profiles between walking with no device vs. the active assistance condition, and the updated MyoSuit [32], which compared angle profiles for each individual subject between walking in a passive knee brace vs. walking with the device in zero-torque mode.

Another option is to eliminate rigid linkages altogether, as in the case of soft exosuits previously developed in our lab which apply propulsive assistance at the ankle and/or the hip. These exosuits securely anchor to the body via textile-based functional apparel components and apply assistive torques by tensioning cables across the target joint(s), and are highly transparent to the user when the cables are slack. Although they have a smaller maximum assistance capability than rigid exoskeletons, they have been shown to still apply sufficient force to demonstrate benefits in both healthy [33]–[37] and clinical [38] populations. This latter approach is the one we adapt in this work for assisting the knee. To the best of our knowledge, the only other published device without potentially restrictive structures at or around the knee was the first version of the MyoSuit [39], which was never evaluated during walking and has since been replaced by a newer version that does have a rigid hinge [32].

In this work, we present a lightweight knee extension exosuit that combines functional apparel with integrated rigid components, which does not have any rigid structure crossing the knee joint. As with previous exosuits, the knee exosuit is highly transparent to the user when unpowered, and this transparency is experimentally validated by comparing angle profiles for individual subjects between the unpowered condition and a no-device baseline. When active, the exosuit can apply up to 36 N·m of torque, approximately half of the peak biological knee extension moment during level walking [40], at any point(s) during the stance phase of gait. While we plan



Fig. 1. Overview of the knee extension exosuit. The exosuit applies knee extension assistance by retracting a Bowden cable across the front of the knee, which is anchored to the body via a thigh wrap and a calf wrap. Additional anchoring of the thigh wrap up the side of the hip to a waist belt limits drift and also results in coupled hip abduction assistance. An inertial measurement unit (IMU) harness with load cells measures applied force and motion data.

to eventually test this device in clinical populations such as post-stroke, in this work we present the device design and discuss the various challenges specific to the knee joint which had to be addressed in adapting the exosuit approach for assisting knee extension. We then demonstrate its use as an experimental platform to systematically explore power-based assistance profiles applied to healthy subjects during incline and decline walking on a treadmill.

II. SYSTEM DESIGN

A. Functional Apparel and Components

The exosuit applies knee extension assistance by tensioning a Bowden cable that crosses in front of the knee. The cable is anchored to the body via two components, a semi-rigid wrap worn around the thigh, and a calf wrap worn around the shank (Fig. 1). When the Bowden cable is retracted, the thigh and calf anchors are pulled closer together, causing the knee to extend. It should be noted that the exosuit anchoring to the body must bear the entirety of the shear load, in contrast to rigid exoskeletons where the load can be borne by the rigid frame and/or transferred to the ground, which is one of the factors behind their lower assistance magnitude.

The calf components consist of a high-grip, cushioning base layer (Fabrifoam, Exton, PA, USA), which is covered by a textile calf wrap with a lightweight rigid frame integrated on the shin. The calf wrap attaches to the base layer and can be securely tightened on the convex geometry of the calf via two adjustment dials (Boa, Denver, CO, USA) near the top and bottom of the wrap. The frame is made of hollow carbon fiber tubing and 3D printed plastic components, and its purpose is to increase the moment arm of the knee exosuit. As the natural moment arm for the knee extensors is small, approximately 4-5 cm [41], this would require very high cable forces to achieve the target levels of assistance, potentially leading

to uncomfortable levels of shear. By extending the moment arm with this frame, the required tension in the exosuit is decreased. While the exact length of the extended moment arm depends on the user's leg anatomy and varies with knee angle, during the stance phase it is approximately 12 cm. The frame also provides cable clearance over the front of the knee. Unlike similar moment arm extenders often seen in ankle devices, which can be attached to the shoe using permanent methods (i.e., drilling into the sole), the calf frame must rest on the surface of the shank. Therefore, it is structured such that normal forces are distributed on either side of the tibial tuberosity via plastic pads, in order to avoid pressure points.

The thigh component is a textile wrap that has been reinforced with a flexible plastic material (Varaform, Runlite, Belgium) to provide structure and limit deformation. Anchoring securely to the thigh is challenging due to the large volume of soft tissue as well as its inverted cone geometry, which is beneficial when pulling upwards, as in the case of hip assistance, but becomes problematic when trying to resist downwards pull during knee assistance. For this reason, the thigh wrap is connected upwards to a waist belt via an additional webbing strap, which helps limit downward drift of the thigh piece. The waist belt itself is resistant to drift as it can anchor onto the bony features of the pelvis.

As this webbing strap crosses the hip joint, knee extension assistance becomes coupled with assistance at the hip, prompting the design choice of how to route the strap. During walking, the hip joint frontal plane moment is primarily abduction for the majority of the stance phase, while the hip sagittal plane moment switches from extension in early stance to flexion in late stance [40]. Since we are primarily interested in providing knee extension assistance during the stance phase, we chose to route this strap along the side of the hip, rather than the front or back, such that the exosuit applies coupled hip abduction assistance rather than hip flexion or extension. This configuration gives the most flexibility for applying various knee extension assistance profiles throughout stance without risking applying moments at the hip that conflict with the normal biological hip moment. This coupling with hip abduction may also complement the knee extension assistance by enhancing synergistic activity for loading of the leg during stance.

Given the goal of using this exosuit in impaired populations such as post-stroke, it is important that it can accommodate a wide range of user sizes and body types. All the wearable components have been designed to be highly adjustable while still allowing for good alignment. The two-piece design of the waist belt enables the lateral straps holding up the thigh wraps to be routed over the trochanters on both sides, independent of waist circumference. The triangular piece on the thigh wrap is attached to the rest of the wrap with a patch of hook-and-loop fastener, and can be shifted laterally to adjust the distance between the Bowden cable anchor point and the connecting strap up to the side of the waist belt. This in turn allows the anchor point to be aligned with the front of the leg, regardless of thigh circumference. The caveat of all this available adjustability is that the person donning the suit must take more care to set the alignment correctly.

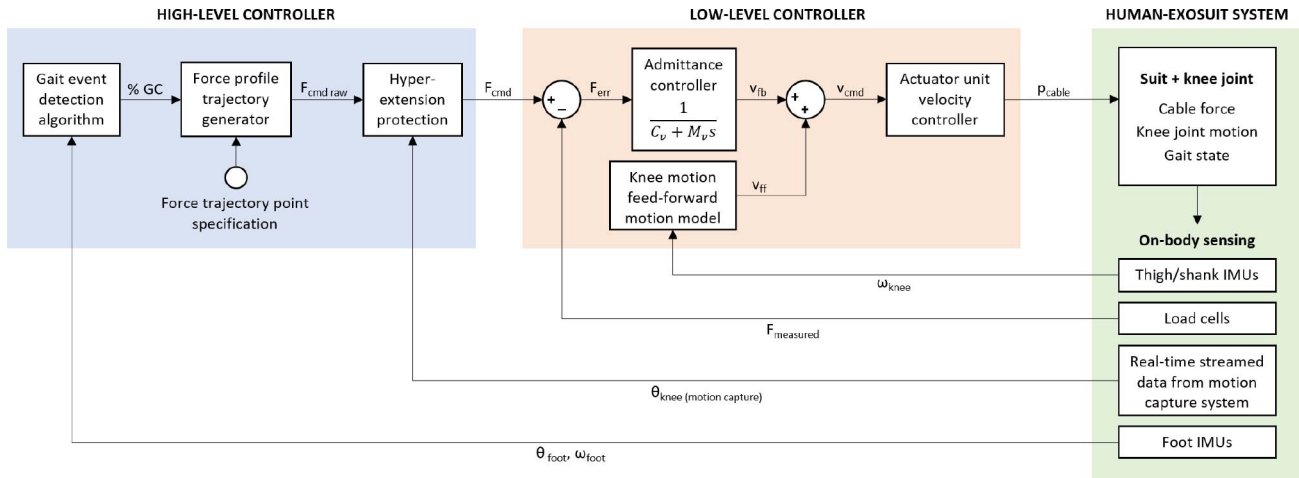


Fig. 2. Diagram of overall controller architecture. At the high level, foot IMU measurements are used to estimate progression through the gait cycle. Based on this estimate, a desired force trajectory is generated in sync with the wearer’s gait cycle. The generated force profile is then modified by the hyperextension protection algorithm, which reduces the force if the wearer is close to maximum allowable knee extension, as determined by motion capture data streaming in real time. This modified force command is sent to the low-level controller, which closes the loop on force using sensor data from an in-line load cell measuring the Bowden cable tension. The admittance controller feedback term is combined with a feed-forward model that compensates for knee motion. The velocity command is sent to the actuator unit which moves the Bowden cable accordingly to apply assistance to the user.

Sensing for the system consists of IMUs (MTi-1, Xsens, Netherlands) on the foot, shank, and thigh of each leg, used for joint angle estimation and gait event detection. In addition, load cells (Futek, Irvine, CA, USA) are placed in-line with the load path at the bottom of the calf wrap to estimate the exosuit-applied assistive moment at the knee. The weight of the components worn by the user is as follows: the waist belt is 375 g, one thigh wrap is 183 g, one calf wrap with liner is 360 g, the IMU harness is 174 g, and one load cell is 43 g. The resulting total mass of the exosuit donned unilaterally is 1.14 kg. The system can be donned bilaterally with an additional thigh wrap, calf wrap, and load cell, in which case the total on-body mass is 1.72 kg.

B. Actuation Unit

The exosuit is tethered to an off-board cart with power, actuation, and control hardware. Mechanical power for the exosuit is generated by a custom actuation unit consisting of two brushless DC motors (Maxon EC-4 pole, maxon motor ag, Switzerland) with 51:1 planetary gearboxes, each of which turn a 40 mm radius, multi-wrap pulley. Forces are transmitted to the exosuit component by the aforementioned Bowden cables. The actuation unit includes a custom electronics board with built-in low-level firmware protections and has a servomotor driver (Gold Twitter, Elmo Motion Control) which tracks a velocity command. Additional detail can be found in [34]. This actuation unit is capable of being worn on the body, but for the experiments presented in this paper, the actuator was situated off-board to minimize the effect of added mass on the participants.

C. Control System Architecture

The main controller is implemented in Simulink Real-Time (MathWorks, Natick, MA, USA) and runs at 1 kHz on a real-time target machine (Speedgoat Inc., Natick, MA, USA).

This target computer interfaces with the actuation unit and the sensors via Controller Area Network (CAN) bus protocol, receiving IMU data at 100 Hz, load cell data at 1 kHz, and sending/receiving motor data and commands at 1 kHz. High-level controller parameters can be modified in real time via the Simulink block diagram on a separate host computer, which is connected to the target via Ethernet. In addition to the exosuit sensors, the controller also receives data streamed in real-time from the laboratory data collection system (Qualisys, Gothenburg, Sweden) over UDP, including motion-capture measured knee angle at 200 Hz and analog data such as ground reaction force (GRF) and surface electromyography (EMG) signals at 1 kHz.

The progression through the gait cycle is estimated from two IMUs on the feet attached onto the lateral side of each shoe below the ankle. The gait detection algorithm is described in detail in [42], and utilizes foot-to-floor angle and angular velocity information to detect key gait events. By using data from both feet, the algorithm has been shown to be robust even in irregular, post-stroke gait [42]. This gait cycle estimate in turn is fed into a trajectory generator that outputs a desired assistance force. Since the optimal profile for knee extension assistance is as yet unknown, we implemented an assistance profile generator that enables highly flexible specification of the force trajectory. The trajectory generator allows a cubic Bezier curve to be defined by multiple control points, with each control point defined by force level, timing within the gait cycle, and desired curvature (Fig. 3).

However, the ability to apply arbitrary assistance profiles to the knee also creates the potential to induce knee hyperextension. Compared to hip and ankle devices where assistance typically begins in the middle of the range of motion and has a large “buffer” until the joint limit, the lower limit of the normal knee angle during stance gets very close to the physical extension limit of the knee joint. As such, having some form of hyperextension protection is necessary. While

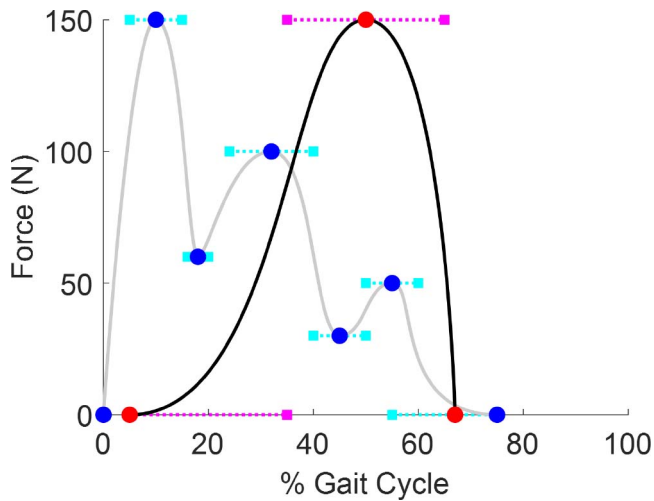


Fig. 3. Force profile generation. The trajectory generator allows a curve to be specified by multiple control points, with each control point (solid dots) defined by force level, timing within the gait cycle, and curvature (indicated by length of dotted lines). This enables highly flexible specification of assistance profiles ranging from simple (black line) to complex (gray line), as seen by the example illustrations of arbitrary profiles shown here.

rigid exoskeletons can simply integrate a mechanical stop into the device joint itself, the hinge-free and soft nature of the knee exosuit makes implementation of such protection challenging. Solutions based on limiting the amount of cable pull work inconsistently, as the distance between the Bowden cable anchor points on the thigh and calf is not fixed: it can vary between participants, between sessions, or even over the course of a single session due to drift.

Our solution is a simple hyperextension protection function in the software, which adjusts the output of the trajectory generator before the assistance profile is applied to the user. The function behaves as a virtual soft stop based on the wearer’s knee angle. If the knee angle goes below a preset “soft limit” threshold, a scaling factor is applied to the force command from the trajectory generator, reducing it proportionally to how close the user is to reaching a hard limit that corresponds to the start of knee hyperextension, typically 0° . For the initial demonstration on the treadmill, the knee angle is measured in real-time via motion capture and streamed to the controller. The streamed knee angle data has an average latency of 15 ms, which is acceptable for the application of walking, which is on the order of 1 Hz. Future embodiments will utilize wearable sensors for knee angle measurements.

The final adjusted force command is sent to the low-level controller, which closes the loop on force using sensor data from an in-line load cell measuring the Bowden cable tension. Stiction in the Bowden cable transmission makes pure force control difficult, so we use an admittance controller, with virtual damping and inertia parameters (C_v and M_v) tuned manually. The admittance controller feedback term is combined with a feed-forward model that compensates for knee motion. The resulting velocity command is then sent to the actuator unit over CAN bus, which then moves the Bowden cable accordingly to apply assistance to the user (Fig. 2).

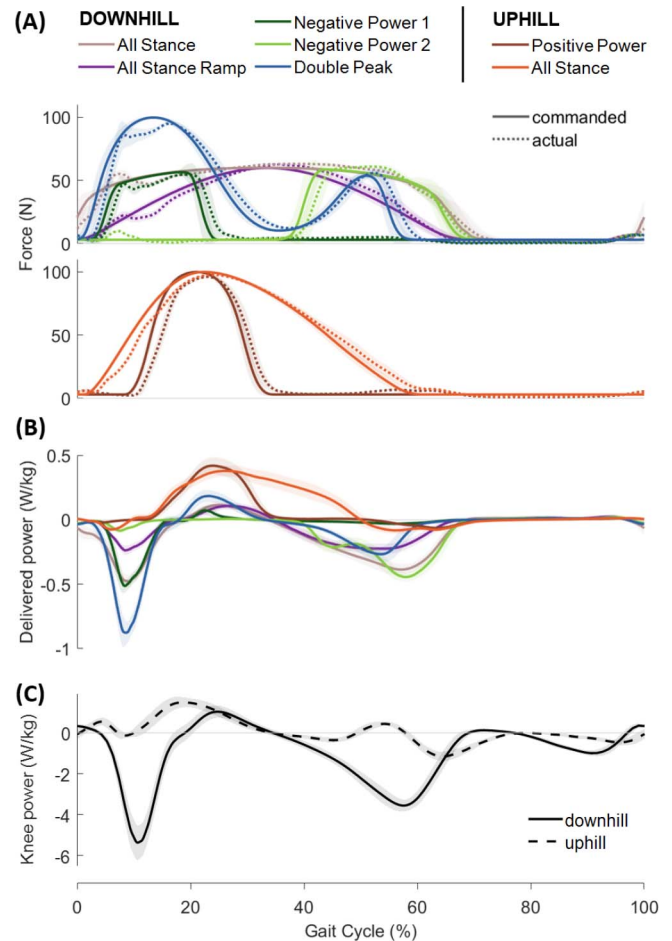


Fig. 4. (A) Assistance force profiles for downhill (top) and uphill (bottom) walking for a representative participant. The force command is the solid line and the measured applied force is the dotted line, showing force tracking performance. (B) The resulting power delivered by the exosuit. (C) Knee joint power profiles from the same representative participant’s exosuit unpowered conditions.

D. Assistance Profiles

While the flexible trajectory generator enables assistance to be applied anywhere in the gait cycle, including in the swing phase, we are primarily interested in applying assistance during the stance phase of walking. For the validation experiments with healthy participants that are presented in this work, we specifically focused on uphill and downhill walking to increase loading on the knee [43], [44] and amplify any effects of applied knee assistance.

The design of the assistance profiles was primarily based on biological knee power profiles during sloped walking (Fig. 4C) [43]. During the stance phase of downhill walking, there are two large negative power regions, separated by a small and brief positive power region in mid-stance: one in early stance corresponding to the knee’s shock absorption role during loading response/weight acceptance, and another in late stance as the body’s center of mass is lowered and the limb braces for push-off [40], [43], [45]. We were interested in the effect of assisting these two negative power regions, both separately in light of their different biomechanical functions, as well as in combination. We tested a “Negative Power 1” (NP1) profile targeting the first negative power region, a “Negative

TABLE I
RMS TRACKING ERROR (MEAN \pm SE) FOR ASSISTANCE PROFILES
NORMALIZED AS A PERCENTAGE OF THE PEAK FORCE

Profile Type	Left	Right
Uphill		
Positive Power	7.19 \pm 1.43	6.21 \pm 0.90
All Stance	6.02 \pm 1.02	5.32 \pm 0.61
Downhill		
All Stance Ramp	7.99 \pm 1.21	6.95 \pm 0.62
All Stance	9.24 \pm 1.49	9.15 \pm 1.57
Negative Power 1	9.35 \pm 0.97	8.88 \pm 1.60
Negative Power 2	9.22 \pm 3.39	9.68 \pm 3.33
Double Peak	8.07 \pm 0.67	7.29 \pm 0.89

Power 2” (NP2) profile targeting the second negative power region, and a “Double Peak” (DP) profile targeting both negative power regions while applying little to no force in the middle positive power region. We also tested an “All Stance” (AS) profile which applied assistance for the entirety of stance. In some participants, we also tested an “All Stance Ramp” (ASR) profile which had a more gradual onset and offset of assistance force for improved subjective comfort.

In uphill walking, the primary feature of the knee joint power profile is a single positive power region in the first half of the stance phase (Fig. 4C), as the knee extends and causes the leg to straighten, raising the body’s center of mass. We tested a “Positive Power” (PP) assistance profile targeting this narrow region. As the sharpness of this profile could be less comfortable for some participants, we also tested a broader version, “Uphill All Stance” (UAS). Fig. 4A-B shows representative examples of all the above profile shapes and the resultant exosuit-delivered power for each.

III. SYSTEM CHARACTERIZATION

A. Force Tracking

The commanded and measured force trajectories for aforementioned assistance profiles on a representative participant are shown in Fig. 4. Table I lists the root mean square (RMS) of the tracking error, defined as the difference between the force command sent to the actuation unit and the actual force measured by the load cell located in-line with the load path at the shank. As the exact assistance profile varied between participants within a given profile type, error values were normalized as a percentage of the peak force of the profile for a given participant.

B. Bi-Articular Assistance Behavior

As discussed in Section II-A, the thigh piece of the exosuit is anchored to the waist via a lateral hip strap. As a result, the exosuit’s load path crosses both the knee and hip joints, such that in addition to the primary target knee extension torque, the exosuit also applies hip abduction torque (Fig. 5). We conducted a single-participant experiment to evaluate the assistive hip abduction torque. An additional load cell was added

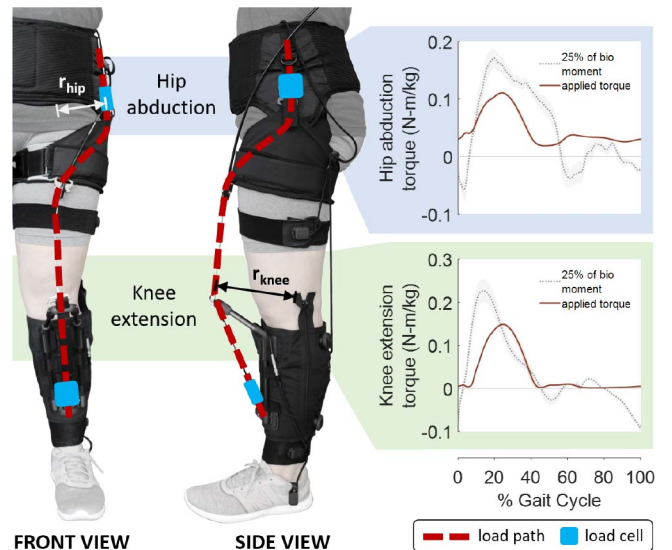


Fig. 5. Front and side views of the exosuit showing the load path in relation to the hip and knee joints (left), and the resulting applied hip abduction and knee extension torque for a representative assistance profile (right). Biological joint moments are overlaid for reference (dotted lines), scaled down by a factor of 4 to fit.

between the waist and thigh exosuit components to measure the tension in the hip strap. Markers were also placed on the strap to estimate the abduction moment arm, which was the frontal plane distance from the strap to the hip joint center. We found that the moment arm for exosuit hip abduction is approximately 12 cm throughout the entire gait cycle for the representative participant. The ratio of peak force at the hip to peak Bowden cable force was approximately 75%, which represents the load distribution between the thigh wrap and waist belt. As the moment arms were similar for both joints, the ratio of hip abduction torque to knee extension torque was equivalent.

C. Hyperextension Protection

To evaluate the performance of the hyperextension protection, we compared the knee angle of a healthy participant walking on a level treadmill with exosuit assistance active, with and without hyperextension protection enabled. For this experiment, the hard limit, e.g., the knee hyperextension threshold below which the exosuit will not apply any force, was set to 0°. The soft limit was adjusted by initially setting it to a large value and slowly decreasing it until the participant felt that the protection was no longer sufficient (Fig. 6A). As seen in Fig. 6B, with the protection off, there were more occurrences of hyperextension compared to with the protection on. The variability of strides increased as well, as seen by the increased range of the minimum knee angle distribution. Interestingly, the mean minimum knee angle is higher, i.e., more flexed, for the protection off condition. This may be the result of the participant adopting a more flexed knee gait as a compensation to reduce the risk of hyperextension.

D. Validation of Transparency

The transparency of the hinge-free exosuit design was evaluated by comparing kinematics for four healthy participants

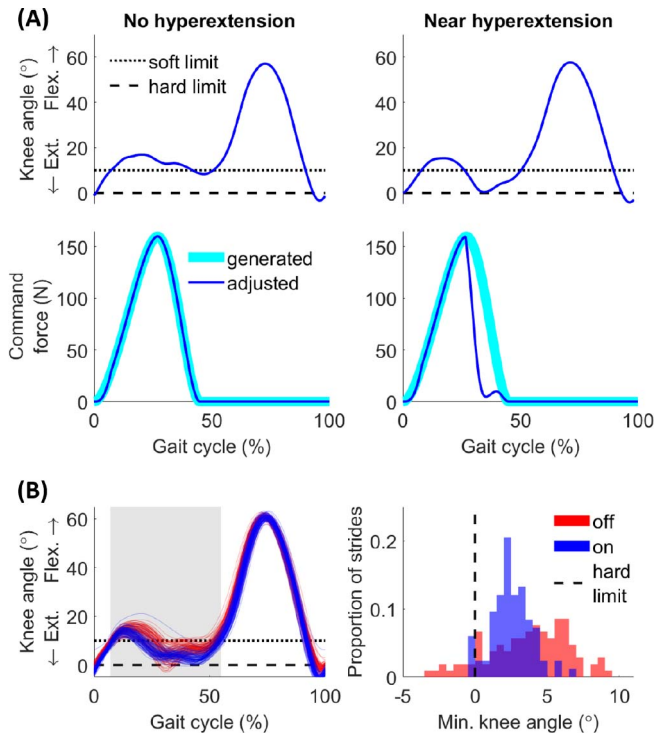


Fig. 6. Soft hyperextension protection. (A) Representative knee joint angle trajectories (top row) of a normal stride (left column) and a stride where the participant approaches hyperextension (right column), and the corresponding force commands (second row). When the knee angle goes below the soft limit, the force command is scaled accordingly, causing it to deviate from the original generated trajectory. (B) Comparison of walking bouts with the protection off vs. on, showing knee angles for all strides and the distribution of the minimum knee angles in the region of interest (grey shaded area).

TABLE II
RMS DEVIATION (MEAN \pm SE $^{\circ}$) BETWEEN NO EXOSUIT AND UNPOWERED EXOSUIT CONDITION SAGITTAL JOINT ANGLES

	Left	Right
Hip	2.7 ± 0.6	2.8 ± 0.9
Knee	1.7 ± 0.3	1.5 ± 0.4
Ankle	0.8 ± 0.2	1.1 ± 0.3

when walking downhill on a treadmill at a 10° decline, without an exosuit compared to with the exosuit donned but unpowered. As seen in Fig. 7, the mean joint angles across participants are very similar between the no exosuit and exosuit unpowered conditions. Table II summarizes the RMS deviation in sagittal joint angles between the two conditions, across four participants. The largest deviation was seen at the hip joint; however, this may be due to the fact that pelvis markers had to be applied atop the waist belt component, which could introduce offsets in the joint angle measurement if the waist belt shifted position over the course of testing. To avoid this issue in the future, reference marks may be made directly on the skin in order to detect the amount of waist belt drift. There were also no statistically significant differences ($p > 0.05$) in the ROM values for all joints between the no-exosuit and unpowered exosuit conditions.

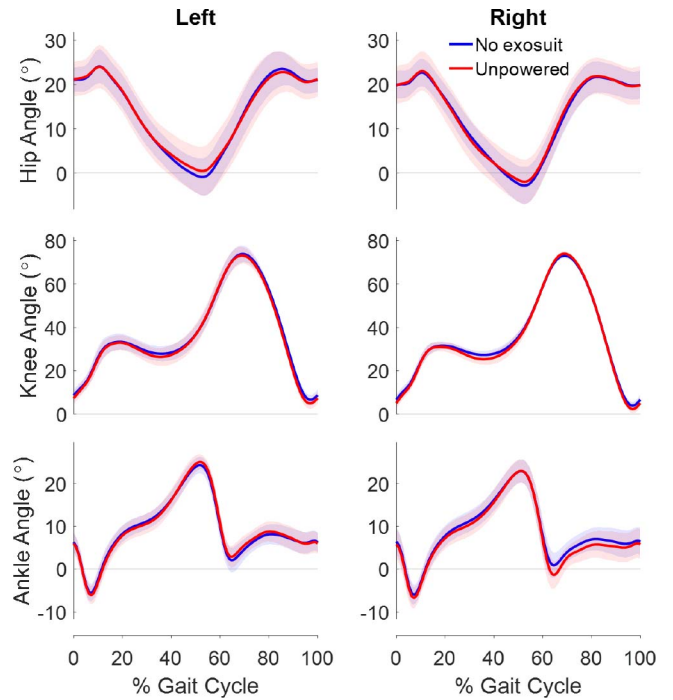


Fig. 7. Evaluation of exosuit transparency. Mean sagittal plane joint angles of $n=4$ participants during downhill walking, without wearing the exosuit vs. wearing the exosuit in unpowered mode. Shaded regions indicate standard error.

IV. HUMAN SUBJECTS TESTING

A. Experimental Protocol

Six healthy individuals with no musculoskeletal injuries participated in this study (age 29.3 ± 3.5 years old, weight 72.0 ± 14.8 kg, height 174.2 ± 10.7 cm, 4 male, 2 female). The study was approved by the Harvard Longwood Medical Area Institutional Review Board and all participants provided written informed consent before their participation.

Each participant came in for two visits on separate days. On both days, each participant walked on a 10° decline and incline at a self-selected fixed comfortable speed (downhill: 1.07 ± 0.10 m/s, uphill: 0.93 ± 0.10 m/s). This slope was selected in order to increase loading on the knee [43], [44], while not being so steep as to induce fatigue within the test session.

The initial visit was a tuning and familiarization session where the subject wore the exosuit and the previously described force profiles were applied. Each profile was then tuned based on subjective feedback from the user. First, the assistance magnitude was increased until the participant indicated it was high enough for small timing changes to be perceptible. Then, onset, offset, and peak timings were adjusted to be earlier or later, also based on subjective feedback. The adjustment of force levels followed by timings was iterated until the participant felt that the assistance provided by a given profile type was as comfortable and helpful as possible. Certain profiles for certain participants were found to be unhelpful or uncomfortable regardless of tuning, and these profiles were removed from a given participant's test set. This

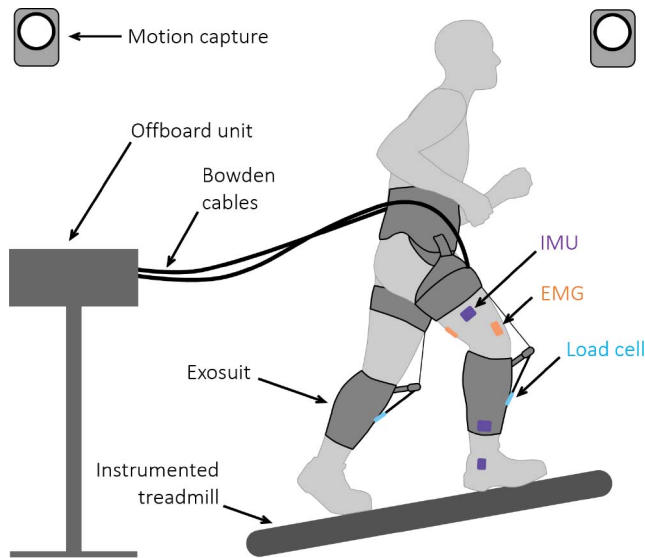


Fig. 8. Illustration of experimental setup and collected measures. Participants walked on a sloped instrumented treadmill at 10° incline and decline while wearing an exosuit tethered to an actuation and control unit located offboard.

manual tuning process allowed for rapid determination of an individualized set of assistance profiles for each participant.

The second visit was a data collection session completed on a separate day. Again, each participant walked uphill and downhill at 10° decline and incline at a self-selected fixed comfortable speed, on an instrumented split-belt treadmill (Bertec, Columbus, OH, USA) as illustrated in Fig. 8. Kinematic data were collected via optical motion capture, using reflective markers placed on anatomical bony landmarks and on cluster plates on the thigh and shank segments for tracking. Additional markers were placed on the exosuit in order to measure the device moment arm. Muscle activity for the following five muscle groups was recorded by wired surface EMG (Bagnoli, Delsys, Natick, MA, USA): rectus femoris (RF), vastus lateralis (VL), vastus medialis (VM), biceps femoris (BF) and gastrocnemius medialis (GM). Electrodes were placed on the dominant leg using SENIAM guidelines [46]. These muscle groups were selected to highlight the influence of assistance on knee extensors (VM, VL, RF) and flexors (BF, GM).

For this session, the tuned profiles from the initial tuning and familiarization session were revisited. In addition to these profiles, “no exosuit” downhill walking and “unpowered exosuit” downhill and uphill walking conditions were also tested as baselines for comparison to active conditions. However, a “no exosuit” uphill walking condition was not included due to experimental time constraints as well as concerns about fatigue due to the strenuous nature of incline walking. For consistency, the data analysis in the remainder of this paper uses the unpowered condition as the baseline for both downhill and uphill walking. Finally, we included a “transparent” condition where a very low, constant cable tension was commanded, to show that the device can actively follow a wearer’s motion as well as to verify that there are no unintended effects such as cueing from motor noise. Incline walking conditions were done last as they were the most fatiguing. Subjects walked

for approximately 4 minutes per condition, with rest breaks between conditions as needed. Two minutes of each condition were recorded for analysis.

B. Data Analysis

Kinematics and kinetics were analyzed using Qualisys and Visual 3D (C-motion Inc., Rockville, MD, USA). Raw marker data were collected from each participant at 200 Hz and GRF and surface EMG measures were collected at 2 kHz. Joint kinematics and kinetics were calculated using participant-specific inverse models, and biological knee moments and powers were calculated by subtracting the torque and power applied by the device from the measured totals. EMG signals were processed to extract average linear envelopes for each gait cycle. Raw EMG signals were filtered with a fourth-order band-pass Butterworth filter with cutoff frequencies of 20–400 Hz in order to remove electrical noise and biological artifacts. Signals were then rectified and low-pass filtered (fourth-order low-pass Butterworth, 12 Hz) to extract corresponding linear envelopes. The EMG amplitude was normalized by the average of corresponding EMG peaks of each participant across conditions. Linear envelopes for each muscle group were segmented (heel strike to consecutive heel strike) and normalized to each gait cycle. The RMS was calculated from each normalized curve for the duration of the condition.

C. Statistical Analysis

For each participant, biological knee joint power and moment measures were normalized with respect to body weight and evaluated by segmentation into early stance (first half of the stance phase), late stance (second half of the stance phase), swing, and total (sum of all three segments). EMG measures were evaluated by the RMS of linear envelopes for each stride. The assistance profiles corresponding to the maximum biological knee joint power reduction of each participant were selected for the group-level analyses. For downhill walking, the profiles achieving this reduction varied across participants. For uphill walking, the “Positive Power” (PP) profile performed the best across all participants, with the exception of one participant for whom PP was the best for one leg, and “Uphill All Stance” for the other. For simplicity, we used PP for all participants for the uphill group-level analysis.

Statistical analysis was conducted with R language [47] using the lme4 package. A linear mixed-effects analysis was done with two factors (powered and unpowered) for each outcome measure to evaluate the effects of the exosuit. For all linear mixed-effect models, subjects were included as random effects. The statistical significance level was set at $\alpha < 0.05$ for all analyses.

V. RESULTS

A. Downhill Negative Power Assistance

Participants reached maximum biological knee power reduction (Fig. 9A) for different negative power assistance profiles: AS ($n = 3$), NP1 ($n = 1$), NP2 ($n = 1$) and DP ($n = 1$)

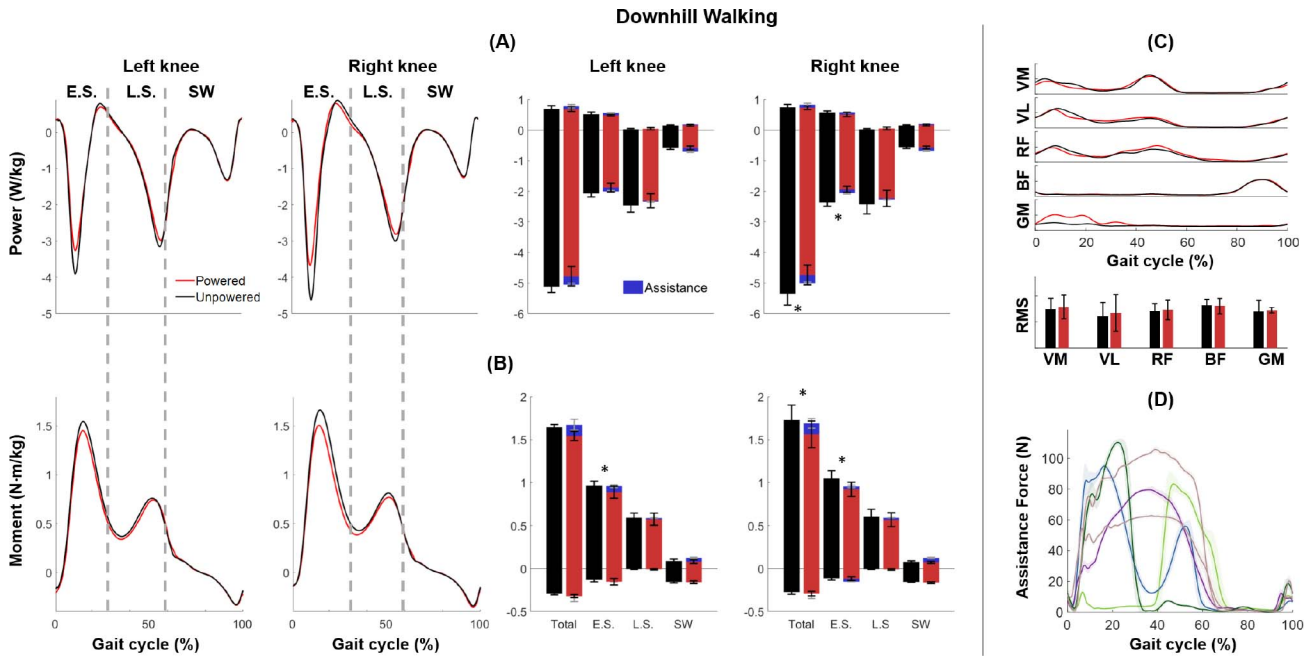


Fig. 9. Downhill walking with unpowered (black) and powered with assistance with maximum biological knee power reduction (red). (A-B) Average knee joint power (A-left) and moment (B-left) trajectories ($n = 6$) segmented into early stance (E.S.), late stance (L.S.), and swing (SW). The average biological knee joint power (A-right) and moment (B-right) for unpowered and powered conditions with delivered assistance by exosuit (blue) during E.S., L.S., SW, and the total sum of the gait segments (mean \pm SE). * indicates $p < 0.05$. (C) Normalized EMG linear envelopes (dominant side) as a percent of the gait cycle for five muscles examined for powered and unpowered conditions for a representative participant (top) and normalized RMS measures (mean \pm SE) across participants throughout each stride (bottom). (D) The assistive force profiles chosen for each participant for group-level analysis of negative power assistance during downhill walking.

(Fig. 9D). Total average negative knee biological power was reduced by $11.4 \pm 0.74\%$ on the right side ($p < 0.001$) and there was a trend for a decrease of $6.73 \pm 5.24\%$ on the left side with no significant difference ($p = 0.207$, Fig. 9B). Total average positive knee biological moment was reduced by $9.70 \pm 2.39\%$ on the right side ($p = 0.011$) and there was a trend for decrease of $6.67 \pm 5.04\%$ on the left side with no significant difference ($p = 0.156$). There was a reduction during early stance in average negative knee power (left: $0.19 \pm 0.09 \text{ W kg}^{-1}$ by $9.53 \pm 4.83\%$, $p = 0.122$, right: $0.43 \pm 0.09 \text{ W kg}^{-1}$ by $17.7 \pm 3.02\%$, $p = 0.001$) and average positive knee moment (left: $0.07 \pm 0.03 \text{ N m kg}^{-1}$ by $8.16 \pm 3.58\%$, $p = 0.041$, right: $0.13 \pm 0.02 \text{ N m kg}^{-1}$ by $12.1 \pm 2.27\%$, $p = 0.005$). The exosuit delivered an average negative power of $0.13 \pm 0.03 \text{ W kg}^{-1}$ and $0.13 \pm 0.02 \text{ W kg}^{-1}$ during early stance for the left and right side, respectively. EMG linear envelopes did not indicate any trends in downhill walking and there were no significant differences in any muscle group ($p > 0.05$, Fig. 9C).

B. Uphill Positive Power Assistance

Positive power assistance (PP, Fig. 10D) during uphill walking resulted in reduced total positive knee biological power (Fig. 10A) on the left side by $17.5 \pm 3.21\%$ ($p = 0.005$) and on the right side by $23.2 \pm 3.54\%$ ($p = 0.008$), and reduced total knee biological moment on the left side by $26.1 \pm 2.28\%$ ($p < 0.001$) and on the right side by $20.8 \pm 3.09\%$ ($p < 0.001$, Fig. 10B). These reductions were mostly driven by early stance reductions in both positive average power (left: $0.23 \pm 0.04 \text{ W kg}^{-1}$ by $29.9 \pm 3.49\%$, $p = 0.003$, right: $0.25 \pm 0.01 \text{ W kg}^{-1}$ by $32.7 \pm 1.45\%$, $p < 0.001$) and positive

average moment (left: $0.15 \pm 0.03 \text{ N m kg}^{-1}$ by $27.8 \pm 3.45\%$, $p = 0.002$, right: $0.13 \pm 0.01 \text{ N m kg}^{-1}$ by $25.6 \pm 2.01\%$, $p < 0.001$). The exosuit delivered positive average power of $0.21 \pm 0.03 \text{ W kg}^{-1}$ and $0.20 \pm 0.02 \text{ W kg}^{-1}$ during early stance for the left and right side respectively. EMG linear envelopes indicated a decreasing trend for the knee extensor quadriceps (RF, VM, VL) throughout the stride but it was not statistically significant ($p > 0.05$, Fig. 10C). No trends were observed in BF and GM ($p > 0.05$).

VI. CONCLUSION AND FUTURE WORK

In this paper, we present the initial development and evaluation of a lightweight, hinge-free exosuit providing knee extension assistance. The hinge-free nature of the exosuit enables it to be highly transparent to the wearer, which was verified by a comparison of joint angle trajectories between “no exosuit” and “unpowered exosuit” conditions. The additional soft limit hyperextension prevention algorithm enabled the application of knee extension assistance without risking inducing knee hyperextension. This algorithm together with the hinge-free design provides complete transparency for knee joint movement during walking, allowing the evaluation of active assistance without confounding mechanical restrictions or limits.

We have implemented a highly flexible spline-based trajectory generator enabling us to command a diverse set of predefined assistance profiles, and demonstrate that we can control the profile of assistance in order to deliver both positive and negative power assistance during walking. The assistance profiles were tuned based on subjective feedback, resulting in individualized profile sets for each participant. The positive power assistance during incline walking resulted in

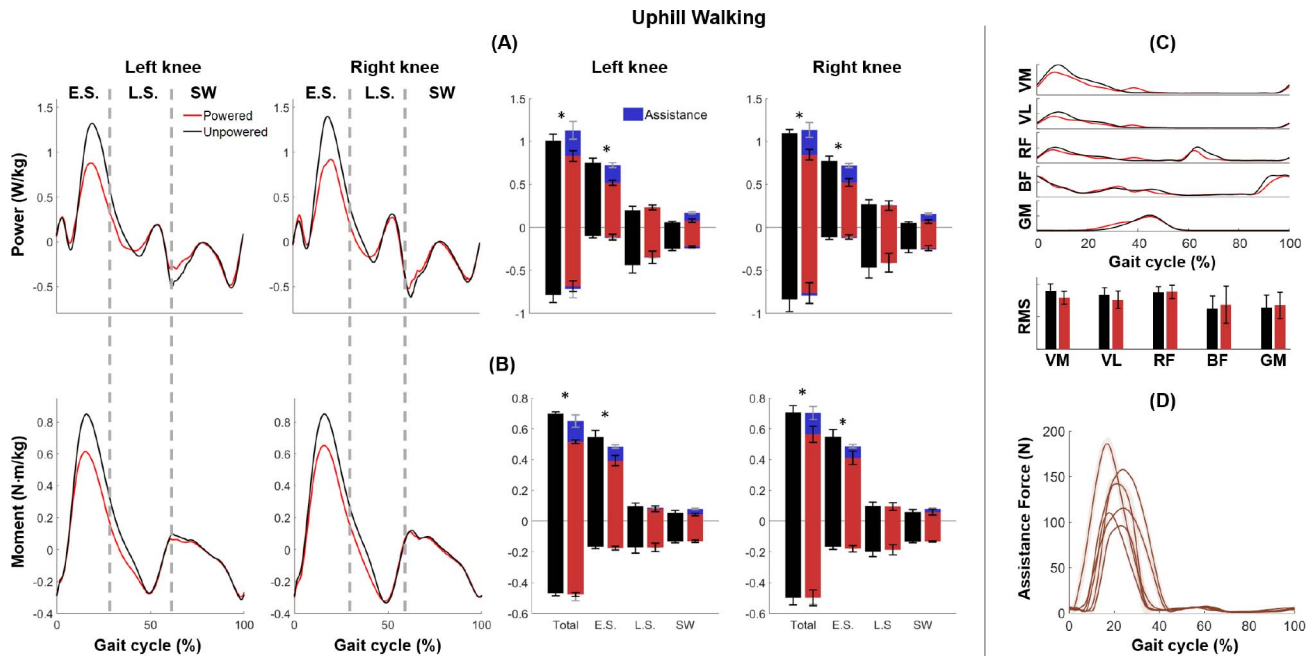


Fig. 10. Uphill walking with unpowered (black) and positive power (PP) assistance (red). (A-B) Average knee joint power (A-left) and moment (B-left) trajectories ($n = 6$) segmented into early stance (E.S.), late stance (L.S.), and swing (SW). The average biological knee joint power (A-right) and moment (B-right) for unpowered and powered conditions with delivered assistance by the exosuit (blue) during E.S., L.S., SW and the total sum of the gait segments (mean \pm SE). * indicates $p < 0.05$. (C) Normalized EMG linear envelopes (dominant side) as a percent of gait cycle for five muscles examined for powered and unpowered conditions for a representative participant (top) and normalized RMS measures (mean \pm SE) across participants throughout the gait cycle (bottom). (D) The assistive force profiles chosen for each participant for group-level analysis of positive power assistance during uphill walking.

significant reduction in the biological knee moment and power, similar to previous observations of positive power augmentation during level walking resulting in reductions at the ankle and hip [35]. In addition, EMG measures indicate a trend of reduced knee extensor muscle activity for uphill walking conditions, but the reductions were not significant at the group level. This discrepancy between the EMG and the moments may indicate that some participants responded to the assistance not by reducing their quadriceps usage, but by altering their walking strategy in some other way. In future experiments, such changes may be possible to detect by collecting EMG measures from a larger set of muscles. For downhill walking, assistance profiles corresponding to maximum biological knee power varied between participants.

Subjective tuning typically led to assistance profiles applying less than the full capacity of the system, i.e., 12–18 N·m of torque out of a total possible 36 N·m. In some cases, this may have stemmed from comfort issues, as increased assistance force leads to increased pressure on the calf. However, it should be noted that most of the participants selected higher peak forces in their uphill assistance profiles compared to their downhill assistance profiles, indicating the perceived assistance during downhill walking might be affected by other factors such as the tradeoff between stability and energy consumption [48], [49] and complexity [50]. It is also possible that participants may need more time to adapt to walking with the knee device before the assistance magnitude can be increased.

Future work will include improvements to the human-device interface and the controller. For example, the current hyperextension prevention implementation, which is in the software only, may not be sufficient at higher forces. In addition, it can only stop the device from pulling the user into

hyperextension, but cannot prevent someone who already hyperextends on their own from doing so. As such, it may be beneficial to integrate some form of hyperextension prevention into the exosuit hardware as well. In addition, for higher levels of applied assistance, it may be important to improve interface comfort and provide means to guarantee proper cable alignment. On the controls side, we are interested in transitioning from the current tethered system to a fully mobile system, implementing more responsive knee angle-based profiles, and making the assistance profile tuning process more systematic by utilizing real-time physiological and biomechanical measures (e.g., online optimization). Our long-term goal is for this knee exosuit to help restore knee function during walking for those with neuromuscular injuries and disorders.

ACKNOWLEDGEMENT

Harvard University has entered into a licensing and collaboration agreement related to the exosuit technology with ReWalk Robotics. Conor J. Walsh is a paid consultant for ReWalk Robotics.

REFERENCES

- [1] T. M. Kepple, K. L. Siegel, and S. J. Stanhope, "Relative contributions of the lower extremity joint moments to forward progression and support during gait," *Gait Posture*, vol. 6, no. 1, pp. 1–8, Aug. 1997.
- [2] J. Perry, J. Burnfield, and J. M. Burnfield, *Gait Analysis: Normal and Pathological Function*. Thorofare, NJ, USA: SLACK, 2010.
- [3] H. M. Abdulhadi, D. C. Kerrigan, and P. J. LaRaia, "Contralateral shoe-lift: Effect on oxygen cost of walking with an immobilized knee," *Arch. Phys. Med. Rehabil.*, vol. 77, no. 7, pp. 670–672, Jul. 1996.
- [4] K.-H. Kong, V.-C. Woon, and S.-Y. Yang, "Prevalence of chronic pain and its impact on health-related quality of life in stroke survivors," *Arch. Phys. Med. Rehabil.*, vol. 85, no. 1, pp. 35–40, 2004.

- [5] M. Bottos and C. Gericke, "Ambulatory capacity in cerebral palsy: Prognostic criteria and consequences for intervention," *Develop. Med. Child Neurol.*, vol. 45, no. 11, pp. 786–790, Feb. 2007.
- [6] M. J. Lomaglio and J. J. Eng, "Muscle strength and weight-bearing symmetry relate to sit-to-stand performance in individuals with stroke," *Gait Posture*, vol. 22, no. 2, pp. 126–131, Oct. 2005.
- [7] A. C. Novak and B. Brouwer, "Kinematic and kinetic evaluation of the stance phase of stair ambulation in persons with stroke and healthy adults: A pilot study," *J. Appl. Biomech.*, vol. 29, no. 4, pp. 443–452, Aug. 2013.
- [8] N. D. Reeves, M. Spanjaard, A. A. Mohagheghi, V. Baltzopoulos, and C. N. Maganaris, "The demands of stair descent relative to maximum capacities in elderly and young adults," *J. Electromyogr. Kinesiol.*, vol. 18, no. 2, pp. 218–227, Apr. 2008.
- [9] S. R. Goldberg, S. Ounpuu, and S. L. Delp, "The importance of swing-phase initial conditions in stiff-knee gait," *J. Biomech.*, vol. 36, no. 8, pp. 1111–1116, Aug. 2003.
- [10] N. D. Neckel, N. Blonien, D. Nichols, and J. Hidler, "Abnormal joint torque patterns exhibited by chronic stroke subjects while walking with a prescribed physiological gait pattern," *J. Neuroeng. Rehabil.*, vol. 5, p. 19, Sep. 2008.
- [11] J. S. Sulzer, K. E. Gordon, Y. Y. Dhaher, M. A. Peshkin, and J. L. Patton, "Preswing knee flexion assistance is coupled with hip abduction in people with stiff-knee gait after stroke," *Stroke*, vol. 41, no. 8, pp. 1709–1714, Aug. 2010.
- [12] K. R. Kaufman, S. E. Irby, J. W. Mathewson, B. W. Wirta, and D. H. Sutherland, "Energy-efficient knee-ankle-foot orthosis: A case study," *J. Prosthet. Orthot.*, vol. 8, no. 3, pp. 79–85, 1996.
- [13] D. C. Kerrigan, H. M. Abdulhadi, T. A. Ribaud, and U. D. Croce, "Biomechanic effects of a contralateral shoe-lift on walking with an immobilized knee," *Arch. Phys. Med. Rehabil.*, vol. 78, no. 10, pp. 1085–1091, Oct. 1997.
- [14] D. J. Farris and G. S. Sawicki, "The mechanics and energetics of human walking and running: A joint level perspective," *J. R. Soc. Interface*, vol. 9, no. 66, pp. 110–118, Jan. 2012.
- [15] S. Galle, P. Malcolm, S. H. Collins, and D. De Clercq, "Reducing the metabolic cost of walking with an ankle exoskeleton: Interaction between actuation timing and power," *J. Neuroeng. Rehabil.*, vol. 14, no. 1, p. 35, 2017.
- [16] S. Lee, S. Crea, P. Malcolm, I. Galiana, A. Asbeck, and C. Walsh, "Controlling negative and positive power at the ankle with a soft exosuit," in *Proc. IEEE Int. Conf. Robot. Autom. (ICRA)*, May 2016, pp. 3509–3515.
- [17] R. W. Jackson and S. H. Collins, "An experimental comparison of the relative benefits of work and torque assistance in ankle exoskeletons," *J. Appl. Physiol.*, vol. 119, no. 5, pp. 541–557, Sep. 2015.
- [18] J. Zhang *et al.*, "Human-in-the-loop optimization of exoskeleton assistance during walking," *Science*, vol. 356, no. 6344, pp. 1280–1284, Jun. 2017.
- [19] P. Malcolm, S. Galle, W. Derave, and D. De Clercq, "Bi-articular Knee-Ankle-Foot exoskeleton produces higher metabolic cost reduction than weight-matched mono-articular exoskeleton," *Front. Neurosci.*, vol. 12, p. 69, Mar. 2018.
- [20] M. R. Tucker, C. Shirota, O. Lambercy, J. Sulzer, and R. Gassert, "Design and characterization of an exoskeleton for perturbing the knee during gait," *IEEE Trans. Biomed. Eng.*, vol. 64, no. 10, pp. 2331–2343, Jan. 2017.
- [21] K. Seo *et al.*, "Adaptive oscillator-based control for active lower-limb exoskeleton and its metabolic impact," in *Proc. IEEE Int. Conf. Robot. Autom. (ICRA)*, 2018, pp. 6752–6758.
- [22] M. K. MacLean and D. P. Ferris, "Energetics of walking with a robotic knee exoskeleton," *J. Appl. Biomech.*, vol. 35, no. 5, pp. 320–326, 2019.
- [23] Z. F. Lerner, D. L. Damiano, and T. C. Bulea, "The effects of exoskeleton assisted knee extension on lower-extremity gait kinematics, kinetics, and muscle activity in children with cerebral palsy," *Sci. Rep.*, vol. 7, no. 1, Oct. 2017, Art. no. 13512.
- [24] D. Zanotto, Y. Akiyama, P. Stegall, and S. K. Agrawal, "Knee joint misalignment in exoskeletons for the lower extremities: Effects on user's gait," *IEEE Trans. Robot.*, vol. 31, no. 4, pp. 978–987, Aug. 2015.
- [25] J. Sinclair, J. Hebron, and P. J. Taylor, "The test-retest reliability of knee joint center location techniques," *J. Appl. Biomech.*, vol. 31, no. 2, pp. 117–121, 2015.
- [26] Z. F. Lerner, D. L. Damiano, H.-S. Park, A. J. Gravuner, and T. C. Bulea, "A robotic exoskeleton for treatment of crouch gait in children with cerebral palsy: Design and initial application," *IEEE Trans. Neural Syst. Rehabil. Eng.*, vol. 25, no. 6, pp. 650–659, Jun. 2017.
- [27] R. Auberger, M. F. Russold, R. Riener, and H. Dietl, "Patient motion using a computerized leg brace in everyday locomotion tasks," *IEEE Trans. Med. Robot. Bionics*, vol. 1, no. 2, pp. 106–114, May 2019.
- [28] H. Choi, K. Seo, S. Hyung, Y. Shim, and S.-C. Lim, "Compact hip-force sensor for a gait-assistance exoskeleton system," *Sensors*, vol. 18, no. 2, p. 566, Feb. 2018.
- [29] S.-H. Lee *et al.*, "Gait performance and foot pressure distribution during wearable robot-assisted gait in elderly adults," *J. Neuroeng. Rehabil.*, vol. 14, no. 1, p. 123, Nov. 2017.
- [30] K. A. Witte, A. M. Fatschel, and S. H. Collins, "Design of a lightweight, tethered, torque-controlled knee exoskeleton," in *Proc. Int. Conf. Rehabil. Robot. (ICORR)*, Jul. 2017, pp. 1646–1653.
- [31] K. Shamaei, M. Cenciarini, A. A. Adams, K. N. Gregorczyk, J. M. Schiffman, and A. M. Dollar, "Design and evaluation of a quasi-passive knee exoskeleton for investigation of motor adaptation in lower extremity joints," *IEEE Trans. Biomed. Eng.*, vol. 61, no. 6, pp. 1809–1821, Jun. 2014.
- [32] F. L. Haufe *et al.*, "User-driven walking assistance: First experimental results using the MyoSUIT," in *Proc. IEEE Int. Conf. Rehabil. Robot.*, Jun. 2019, pp. 944–949.
- [33] B. T. Quinlivan *et al.*, "Assistance magnitude versus metabolic cost reductions for a tethered multiarticular soft exosuit," *Sci. Robot.*, vol. 2, no. 2, Jan. 2017, Art. no. eaah4416.
- [34] J. Kim *et al.*, "Autonomous and portable soft exosuit for hip extension assistance with online walking and running detection algorithm," in *Proc. IEEE Int. Conf. Robot. Autom. (ICRA)*, May 2018, pp. 1–8.
- [35] S. Lee *et al.*, "Autonomous multi-joint soft exosuit with augmentation-power-based control parameter tuning reduces energy cost of loaded walking," *J. Neuroeng. Rehabil.*, vol. 15, no. 1, p. 66, Jul. 2018.
- [36] S. Lee *et al.*, "Autonomous multi-joint soft exosuit for assistance with walking overground," in *Proc. IEEE Int. Conf. Robot. Autom. (ICRA)*, May 2018, pp. 2812–2819.
- [37] F. A. Panizzolo *et al.*, "A biologically-inspired multi-joint soft exosuit that can reduce the energy cost of loaded walking," *J. Neuroeng. Rehabil.*, vol. 13, no. 1, p. 43, May 2016.
- [38] L. N. Awad *et al.*, "A soft robotic exosuit improves walking in patients after stroke," *Sci. Trans. Med.*, vol. 9, no. 400, Jul. 2017, Art. no. eaai9084.
- [39] K. Schmidt *et al.*, "The myosuit: Bi-articular anti-gravity exosuit that reduces hip extensor activity in sitting transfers," *Front. Neurobot.*, vol. 11, p. 57, Oct. 2017.
- [40] D. A. Winter, *Biomechanics and Motor Control of Human Movement*. Hoboken, NJ, USA: Wiley, 2009.
- [41] J. L. Krevolin, M. G. Pandy, and J. C. Pearce, "Moment arm of the patellar tendon in the human knee," *J. Biomech.*, vol. 37, no. 5, pp. 785–788, 2004.
- [42] J. Bae *et al.*, "A lightweight and efficient portable soft exosuit for paretic ankle assistance in walking after stroke," in *Proc. IEEE Int. Conf. Robot. Autom. (ICRA)*, May 2018, pp. 2820–2827.
- [43] N. Alexander, G. Strutzenberger, L. M. Ameshofer, and H. Schwameder, "Lower limb joint work and joint work contribution during downhill and uphill walking at different inclinations," *J. Biomech.*, vol. 61, pp. 75–80, Aug. 2017.
- [44] A. N. Lay, C. J. Hass, and R. J. Gregor, "The effects of sloped surfaces on locomotion: A kinematic and kinetic analysis," *J. Biomech.*, vol. 39, no. 9, pp. 1621–1628, 2006.
- [45] J. Rose and J. Gamble, *Human Walking* (LWW Medical Book Collection). Philadelphia, PA, USA: Lippincott Williams & Wilkins, 2006.
- [46] B. Freriks, H. J. Hermens, C. Disselhorst-Klug, and G. Rau, "The recommendations for sensors and sensor placement procedures for surface ElectroMyoGraphy," Roessingh Res. Develop., Enschede, The Netherlands, Rep. RWTH-CONV-097787, 1999.
- [47] *R: A Language and Environment for Statistical Computing*, R Develop. Core Team, Vienna, Austria, 2013.
- [48] L. C. Hunter, E. C. Hendrix, and J. C. Dean, "The cost of walking downhill: Is the preferred gait energetically optimal?" *J. Biomech.*, vol. 43, no. 10, pp. 1910–1915, Jul. 2010.
- [49] E. D. Monsch, C. O. Franz, and J. C. Dean, "The effects of gait strategy on metabolic rate and indicators of stability during downhill walking," *J. Biomech.*, vol. 45, no. 11, pp. 1928–1933, Jul. 2012.
- [50] M. F. Vieira, F. B. Rodrigues, G. S. de Sá E Souza, R. M. Magnani, G. C. Lehnen, and A. O. Andrade, "Linear and nonlinear gait features in older adults walking on inclined surfaces at different speeds," *Ann. Biomed. Eng.*, vol. 45, no. 6, pp. 1560–1571, Jun. 2017.